

Two-Dimensional T₁-T₂ Encoded Pulse Sequence Development at 0.064T

Ella Wilczynski¹, Nathan H. Williamson^{1,2}, Alexandru V. Avram¹, Francesco Padormo³, and Peter J. Basser¹

¹Section on Quantitative Imaging and Tissue Sciences (SQITS), National Institute of Child Health and Human Development (NICHD), National Institutes of Health (NIH), Bethesda, MD, United States, ²Military Traumatic Brain Injury Initiative (MTBI2), Henry M. Jackson Foundation (HJF) for the Advancement of Military Medicine, Bethesda, MD, United States, ³Hyperfine, Inc. Guilford, CT USA, Guilford, CT, United States

Synopsis

Keywords: Low-Field MRI, Low-Field MRI, Phantom, ultra-low field MRI

Motivation: Advancing the capabilities to characterize tissue microstructure on ultra-low field (ULF) MRI scanners enables large-scale longitudinal studies of brain developmental trajectories in normal and diseased pediatric populations.

Goal(s): To develop and vet new multi-dimensional MRI (mdMRI) sequences and processing pipelines for use in following brain developmental trajectories in pediatric subjects, which has never been demonstrated previously on ultralow-field MRI scanners.

Approach: We design, implement, and vet mdMRI pulse sequences on an ULF MRI scanner using quantitative diffusometry and relaxometry MRI phantoms.

Results: Good progress has been made migrating multi-dimensional MRI methods developed for high-field to ULF MRI scanners, which poses many challenges.

Impact: Little is known about healthy brain development of children in LMICs, where there is limited access to radiology. This project intends to improve our understanding of determinants of brain health and help democratize access to radiological resources worldwide.

Introduction

There is a growing interest in using ultra-low field (ULF) MRI scanners¹, particularly in low to middle income countries (LMICs), e.g., to improve neonatal care and characterize neurodevelopment². Multi-dimensional MRI is used in high-field scanners, providing relaxometry-diffusometry spectra to probe distinct water pools in tissues, particularly in the brain. The technique uses images acquired with multiple contrast encodings simultaneously, to quantify the correlation spectrum of MR-sensitive biophysical tissue properties in each voxel^{3,4}. This methodology, to date, has not been migrated to ULF scanners. Critical quantitative tools to enable this translation are MRI phantoms containing “standards” to validate these sequences. However, to date, none of these phantoms has provided standards for ULF scanners, although some data is available here⁵. This work describes efforts to migrate multi-dimensional MRI methods to a Hyperfine 64 mT MRI scanner, specifically the development of 2D T₁-T₂ spectral imaging, and advance sequence validation using a CaliberMRI phantom.

Methods

Measurements were conducted on a 0.064T Hyperfine Swoop MRI scanner (hardware 1.8, software rc8.8.0_Beta1, Guilford CT, USA) using an 8-channel receive, and a 1-channel transmit RF coil.

A saturation-recovery 3D fast spin echo SR-FSE sequence was developed, to allow for two-dimensional spectral encoding of data on this ULF scanner (Fig. 1). The choice of saturation pulse was designed to avoid magnetization transfer effects. Images were acquired with a 2 mm² in-plane resolution and 5 mm slice thickness, with a field of view of 18 cm × 18 cm × 10 cm and TE/TR=4.92/7500 ms.

The acquisition scheme was designed to maximize the accuracy of TE values, by choosing only 2 echo averages per k-space line. It included 4 dummy scans and oversampling factor of 4, to increase SNR. Scans were conducted with 64 re-phasing pulses, yielding 32 echoes (due to 2-echo averaging): 9.84:9.84:314.88 ms, and 32 different saturation times of: 27, 32, 38, 45, 60, 70, 80, 90, 100, 200, 300, 400, 500, 600, 700, 800, 900, 1000, 1200, 1400, 1600, 1800, 2000, 2500, 3000, 3500, 4000, 4500, 5000, 5500, 6000, 7000 ms, and an additional scan with no saturation pulse.

We scanned the CaliberMRI Mini Hybrid Phantom (CaliberMRI, Boulder, CO, USA), containing polyvinylpyrrolidone (PVP), MnCl₂ and NiCl₂ in various concentrations (Fig. 2a).

Analysis

T₁ and T₂ maps were calculated, both separately, by fitting to the following equation (R²>0.9):

$$S(TS, TR) = S_0 \left(1 - \exp\left(-\frac{TS}{T_1}\right) + \exp\left(-\frac{TR}{T_1}\right) \right); S(TE) = S_0 \exp\left(-\frac{TE}{T_2}\right)$$

respectively, and jointly, by assuming single components, which is appropriate in this phantom, using the equation:

$$S(TS, TR, TE) = S_0 \left(1 - \exp\left(-\frac{TS}{T_1}\right) + \exp\left(-\frac{TR}{T_1}\right) \right) \exp\left(-\frac{TE}{T_2}\right)$$

Two dimensional non-parametric ILT spectral analysis was employed in ROIs of five PVP concentrations (the outer ring of tubes). Spectra were computed for both T₁ and T₂ using Tikhonov regularization and singular value decomposition⁶ and plotted on a log₁₀-spaced grid. The analysis here used a ILT version routine developed by Callaghan and colleagues⁷.

Results

In Figure 2 the jointly calculated T₁ and T₂ maps are shown, using ROIs segments, based on the phantom diagrams.

Figure 3 displays the joint T₁ and T₂ parameters in each tube averaged per ROI (mean±SD), only in the outer ring of the phantom.

In Figure 4a, the results of the 2D spectral analysis of the sum of signal from five PVP concentrations are shown. The values of T_1 and T_2 at the peak point of the spectrum are plotted as a function of concentration in Figure 4c.

Discussion

There is good agreement between the separate T_1 and T_2 analyses (not shown) and the joint analysis shown in Figures 2&3. At this low field T_1 and T_2 values are very similar. Measured T_1 's are shorter, and T_2 's are longer than those measured at high B_0 field using conventional clinical MRI scanners. MnCl₂ and NiCl₂ results show a clearer monotonic behavior than PVP, especially for T_2 (Fig. 3). This is also evident by the variation in PVP tubes, as shown in Fig. 2. This might be due insuicently long TE values to measure these long T_2 attenuations. Value differences are also evident when comparing tubes with water in various positions in the phantom, hinting on B_0 and B_1 inhomogeneity. The 2D-ILT spectral analysis mostly showed a single peak, as predicted for the separate tubes, with similar values of T_1 and T_2 , as with the joint T_1 - T_2 fitting model.

Conclusions

This study shows the promise of a new multi-dimensional MRI sequence development for ULF portable scanners. Further improvement of pulse design, parameters optimization and scan durations are planned.

Acknowledgements

We wish to acknowledge the Intramural Research Program of the Eunice Kennedy Shriver National Institute of Child Health and Human Development, the Gates Foundation, the UNITY Consortium, and the Military Traumatic Brain injury Initiative for supporting different aspects of this study.

References

1. Padormo, F., Cawley, P., Dillon, L., Hughes, E., Almalbis, J., Robinson, J., ... & Hajnal, J. V. (2023). In vivo T_1 mapping of neonatal brain tissue at 64 mT. *Magnetic resonance in medicine*, 89(3), 1016-1025.
2. Abate, F., Adu-Amankwah, A., Ae-Ngibise, K. A., Agbokey, F., Agyemang, V. A., Agyemang, C. T., ... & Williams, S. C. R. (2024). UNITY: A low-field magnetic resonance neuroimaging initiative to characterize neurodevelopment in low and middle-income settings. *Developmental Cognitive Neuroscience*, 69, 101397.
3. Benjamini, D., & Basser, P. J. (2016). Use of marginal distributions constrained optimization (MADCO) for accelerated 2D MRI relaxometry and diffusometry. *Journal of magnetic resonance*, 271, 40-45.
4. Avram, A. V., Sarlls, J. E., & Basser, P. J. (2021). Whole-brain imaging of subvoxel T_1 -diffusion correlation spectra in human subjects. *Frontiers in Neuroscience*, 15, 671465.
5. Jordanova, K. V., Martin, M. N., Ogier, S. E., Poorman, M. E., & Keenan, K. E. (2023). In vivo quantitative MRI: T_1 and T_2 measurements of the human brain at 0.064 T. *Magnetic Resonance Materials in Physics, Biology and Medicine*, 36(3), 487-498.
6. Song, Y. Q., Venkataramanan, L., Hürlimann, M. D., Flaum, M., Frulla, P., & Straley, C. (2002). T_1 - T_2 correlation spectra obtained using a fast two-dimensional Laplace inversion. *Journal of Magnetic Resonance*, 154(2), 261-268.
7. Godefroy, S., & Callaghan, P. T. (2003). 2D relaxation/diffusion correlations in porous media. *Magnetic Resonance Imaging*, 21(3-4), 381-383.

Figures

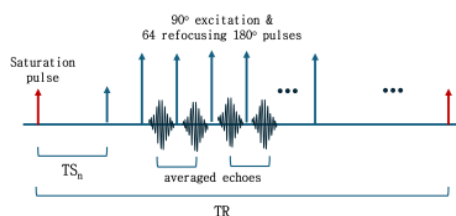


Fig. 1: Pulse-sequence diagram of Saturation-Recovery 3D fast spin echo. The sequence consists of a saturation pulse, a multi echo output train with 2 echo-averaging and multiple repetitions with varying saturation times (TS).

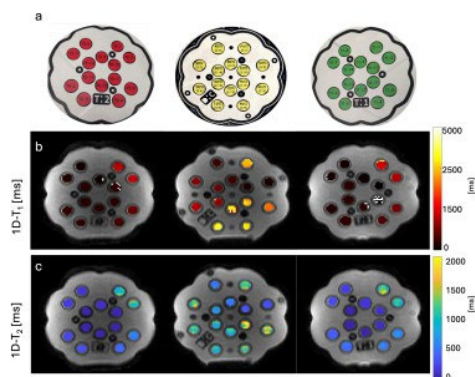


Fig. 2: (a) depicts 3 layers of the phantom containing MnCl₂, PVP and NiCl₂, respectively, each with 14 tubes containing different concentrations. (b) and (c) are the joint analysis of T₁ and T₂ maps (respectively) estimated in each pixel.

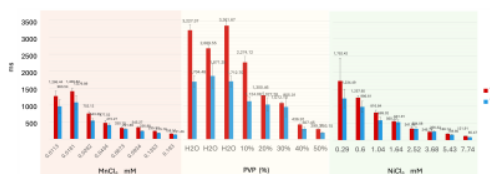


Fig. 3: T₁ and T₂ values (red and blue, respectively) averaged over (mean±SD) each tube of concentration (mean±SD), in all three slices denoted by background color: orange – MnCl₂, yellow – PVP and green – NiCl₂. Values appear at the edge of each bar.

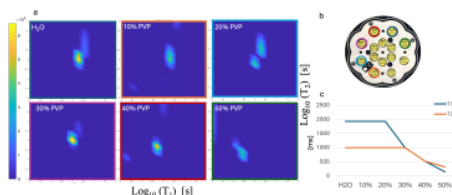


Fig. 4: (a) 2D spectral representation of T₁ and T₂ in a logarithmic scale. Subplot represent the sum of signal from 5 tubes of PVP, denoted by colors in subplot (b). (c) shows the peak values of T₁ and T₂ as a function of concentration.